Microsyst Technol (2017) 23:2561–2568
DOI 10.1007/s00542-016-2988-y

TECHNICAL PAPER

The effect of nonlinear elasticity on the large amplitude free vibration behavior of elastic plates at small scale

S. Zeng[1] · B. L. Wang[1,2]

Received: 19 March 2016 / Accepted: 13 May 2016 / Published online: 8 June 2016

Abstract The effect of nonlinear elasticity on the free vibration behavior of elastic plates has been evaluated by employing continuum mechanics model. The second-order non-linear stress–strain relationship has been considered and the Kirchhoff's hypothesis has been applied on the elastic plate. The large deformation during vibration has also been considered. By using the Hamilton principle, the governing equations of the free vibration of the plate under different boundary condition have been obtained. In order to get the explicit solutions of the governing equations, the Galerkin's method and the harmonic balance method have been utilized. The relationship between the vibration frequency and the vibration amplitude has been discussed and the vibration frequencies of different shaped plate have been compared. It is perceived that the nonlinear elasticity has a distinct effect on the free vibration of the plate.

1 Introduction

Plate-like nanostructures are widely applied in biosensors, biomechanical organs, micro-actuators, micro-switches and vibration sensors (Sahmani and Bahrami 2015; Arani et al. 2013; Ansari et al. 2012). They have wide applications and have attracted many studies for their vibrational behavior. Behfar and Naghdabadi (2005) investigated the nanoscale vibration behavior of a multilayered graphene sheet embedded in an elastic medium and determined the corresponding natural frequencies and the associated modes. Yang and Lim (2009) studied the nonlinear free vibrations of a nano-beam with simply supported boundary conditions based on nonlocal elasticity theory. Nonlinear free vibration of single-walled carbon nanotubes based on the Timoshenko beam model was studied by Yang et al. (2010). Jomehzadeh and Saidi (2011) developed a Navier solution for vibration analysis of nano-plates using three-dimensional nonlocal elasticity theory.

Micro-/nano-structures are extremely small. Under external mechanical load, they may experience significant deformation. Therefore, the study of large amplitude vibration of such small structures is necessary. Wang and Wang (2012) considered the influence of surface effects for the large amplitude vibration of nano scale plates. Ghayesh and Farokhi (2015) discussed different response amplitudes of the nonlinear dynamics of a micro-plate based on the modified couple stress theory. Farokhi and Ghayesh (2015) examined the nonlinear dynamical behavior of a geometrically imperfect micro-plate based on the modified couple stress theory. Asghari (2012) modeled the geometrically nonlinear micro-plate formulation based on the modified couple stress theory.

On the other hand, large deformation of the micro-/nano- structures may result in their nonlinear elasticity behavior. For example, Xiao et al. (2004) investigated nonlinear elasticity and elastic instability of single-walled carbon nanotubes under large-scale axial compression by molecular simulations using the second-generation Brenner potential. Recently, Lee et al. (2008) measured the nonlinear elastic stress–strain response and intrinsic braking strength of free-standing monolayer graphene membranes by nano-indentation experiment. They interpreted that the force–displacement behavior is within a framework of second order elastic stress–strain response. Cadelano et al.

✉ S. Zeng
shan_tzeng@sina.com

[1] Graduate School at Shenzhen, Harbin Institute of Technology, Harbin 150001, People's Republic of China

[2] Institute for Infrastructure Engineering, Western Sydney University, Penrith, NSW 2751, Australia

(2009) developed the Lee et al.'s second order constitutive model, derived the corresponding strain energy function, and imposed the symmetry to reduce the number of independent fitting coefficients. The approach of Sfyris et al. (2014) uses the classical theory of invariant to describe graphene at the continuum level. The work of Wei et al. (2009) expands the analysis of Cadelano et al. by using a fifth order elasticity framework.

Based on the literature reviewing, we noted that micro/nano scale plates were not investigated under the consideration of large deformation and nonlinear elasticity. Yet, large deformation and nonlinear elasticity can happen simultaneously for such small plates. In this paper, the effect of nonlinear elasticity on the free vibration of elastic plates is evaluated by incorporating the second-order nonlinear stress–strain relationship into the classical Kirchhoff plate theory with consideration of large deformation. By using the Hamilton's principle, the governing equations of the free vibration of the graphene sheet under different boundary condition are obtained. Afterward, the Galerkin's method and the harmonic balance method are employed to obtain the explicit solutions of the governing equations along with simply supported and clamped edge supports. The vibration frequency for different aspect ratio for simply supported and rigidly clamped graphene sheet has also been studied.

2 Theoretical formulation

Shown in Fig. 1 is the geometry of a nano-plate in Cartesian coordinates (x, y, z). h denotes the thickness and a, b denote the length and width, respectively. The thickness of the plate is small compared with the length and width, hence Kirchhoff's hypothesis may be assumed to be valid. The displacement components u_x, u_y, u_z are $u_x = -z\frac{\partial w}{\partial x}$, $u_y = -z\frac{\partial w}{\partial y}$, $u_z = w$, where w is the transverse deflection at $z = 0$.

To study the nonlinear elasticity of the plate, we approximate the force–deformation relationship as a nonlinear phenomena scalar connection between the stress (σ) applied and the observed strain (ε), $\sigma = E\varepsilon + D\varepsilon^2$, in which E and D are Young's modulus of elasticity's modulus and an effective non-linear (third-order) of two-dimensional carbon sheets. We follow the stain energy function U_e proved by Cadelano et al. (2009) considering the strain energy function is invariant under a rotation about the z axis of π/3. The expression is as follows:

$$2U_e = \frac{E}{1+\upsilon}\varepsilon_{\alpha\alpha}\varepsilon_{\beta\beta} + \frac{E\upsilon}{1-\upsilon^2}\varepsilon_{\alpha\beta}^2 + \Lambda_1\left(\varepsilon_{\alpha\alpha}^3 + \varepsilon_{\beta\beta}^3\right) + \Lambda_2\varepsilon_{\alpha\alpha}\varepsilon_{\beta\beta}\varepsilon_{\alpha\beta} + \Lambda_3\varepsilon_{\alpha\beta}^3, \tag{1}$$

where E and υ denote the two-dimensional Young's modulus and Poisson's ratio, ε is the strain tensor ($\alpha\ \beta = x, y$) and Λ_i ($i = 1, 2, 3$) are three nonlinear independent elastic coefficients, which are given by

$$\Lambda_1 = C_{111} - C_{222}, \tag{2a}$$

$$\Lambda_2 = \frac{1}{4}(C_{222} - C_{112}), \tag{2b}$$

$$\Lambda_3 = \frac{1}{12}(2C_{111} - C_{111} + 3C_{112}), \tag{2c}$$

where $C_{111}, C_{222}, C_{112}$ are third-order elastic constants, which are defined in crystal elasticity. The elastic moduli in two perpendicular orientations of plates are different due to armchair or zigzag configurations (Jomehzadeh and Saidi 2011). However, if exchange x and y in Eq. (1), we find that the strain energy remains the same. Therefore the employment of combining the Kirchhoff hypothesis and the von-Karman assumption together with Eq. (1) is reasonable on the armchair or zigzag direction. Substitute Eqs. (2a–2c) into Eq. (1), and expand the last three term of Eq. (1), the strain energy function are obtained

$$\begin{aligned} 2U_e = {} & \frac{E}{1+\upsilon}\varepsilon_{\alpha\alpha}\varepsilon_{\beta\beta} + \frac{E\upsilon}{1-\upsilon^2}\varepsilon_{\alpha\beta}^2 \\ & + \frac{1}{3}C_{111}\varepsilon_{xx}^3 + \frac{1}{3}C_{222}\varepsilon_{yy}^3 + C_{112}\varepsilon_{xx}^2\varepsilon_{yy} \\ & + (C_{111} - C_{222} + C_{112})\varepsilon_{xx}\varepsilon_{yy}^2 \\ & + (3C_{222} - 2C_{111} - C_{112})\varepsilon_{xx}\varepsilon_{xy}^2 \\ & + (2C_{111} - C_{222} - C_{112})\varepsilon_{yy}\varepsilon_{xy}^2. \end{aligned} \tag{3}$$

We can see that the first two terms of the right hand side of above equation implicate the linear stain energy density, while the other terms demonstrate the nonlinear behavior. According to Von Karman plate theory, the strain yields

$$\varepsilon_{xx} = -zw_{,xx} + \frac{1}{2}w_{,x}^2, \tag{4a}$$

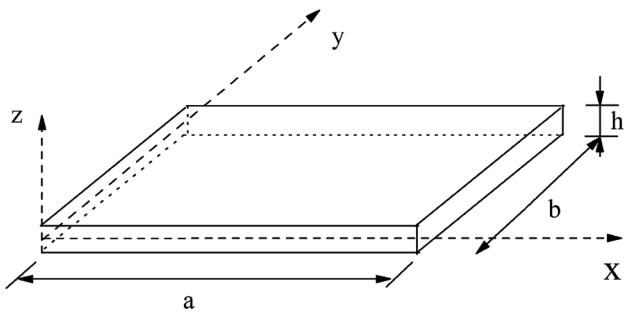

Fig. 1 Geometry of a graphene nano-plate

$$\varepsilon_{yy} = -zw_{,yy} + \frac{1}{2}w_{,y}^2, \tag{4b}$$

$$\varepsilon_{xy} = -zw_{,xy} + \frac{1}{2}w_{,x}w_{,y}, \tag{4c}$$

$$\varepsilon_{xz} = \varepsilon_{zz} = \varepsilon_{yz} = 0, \tag{4d}$$

where $()_{,i}$ denotes the partial differentiation with respect to i coordinate. Substitute Eqs. (4a–4d) into Eq. (3) and integrate the strain energy function on the body of the plate, and ignore the h^3 terms coupling with the nonlinear elasticity, we obtain

$$\begin{aligned} 2U = \int_{-\frac{h}{2}}^{\frac{h}{2}} \iint 2U_e dxdydz = \int_A \Bigg\{ & \frac{Eh}{1-\upsilon^2}\left(\frac{1}{4}w_{,x}^4 + \frac{1}{4}w_{,y}^4 + \frac{1}{2}w_{,x}^2 w_{,y}^2\right) \\ & + \frac{Eh^3}{12(1+\upsilon)}\left(w_{,xx}^2 + w_{,yy}^2 + 2w_{,xx}w_{,yy}\right) \\ & + \frac{Eh^3\upsilon}{12(1-\upsilon^2)}\left(w_{,xx}^2 + w_{,yy}^2 + 2w_{,xy}^2\right) \\ & + \frac{h}{24}C_{111}w_{,x}^6 + \frac{h}{24}C_{222}w_{,y}^6 + (3C_{222} - 2C_{111})\frac{h}{8}w_{,x}^4 w_{,y}^2 \\ & + (3C_{111} - 2C_{222})\frac{h}{8}w_{,x}^2 w_{,y}^4 \Bigg\} dxdy. \end{aligned} \tag{5}$$

The kinetic energy of the plate is given by

$$V = \iint_A \frac{m}{2}\left[h\dot{w}^2 + \frac{h^3}{12}\left(\dot{w}_{,x}^2 + \dot{w}_{,y}^2\right)\right] dxdy, \tag{6}$$

where m is the mass density of the plate, and $\dot{w}$ denotes the partial differentiation with respect to time. In order to obtain the governing equation for the free vibration of the plate, the Hamilton principle is used here. The principle takes the following form,

$$\delta \int_{t_0}^{t_1} (V - U)dt = 0, \tag{7}$$

where t_0 and t_1 are two arbitrary times, and δ denotes the variation operator. By substituting Eqs. (5, 6) into Eq. (7), we obtain the governing equations

$$\begin{aligned} & \mathcal{A}_{,x} + \mathcal{B}_{,y} - \mathcal{C}_{,xx} - \mathcal{D}_{,yy} - \mathcal{F}_{,xy} - mh\ddot{\omega} + m\frac{h^3}{12}\ddot{\omega}_{,xx} \\ & \quad + m\frac{h^3}{12}\ddot{\omega}_{,yy} = 0, \end{aligned} \tag{8}$$

where

$$\begin{aligned} \mathcal{A} = & \frac{Eh}{2(1-\upsilon^2)}\left(w_{,x}^3 + w_{,x}w_{,y}^2\right) + \frac{(3C_{222} - 2C_{111})h}{4}w_{,x}^3 w_{,y}^2 \\ & + \frac{h}{8}C_{111}w_{,x}^5 + \frac{(3C_{111} - 2C_{222})h}{8}w_{,x}w_{,y}^4, \end{aligned} \tag{9a}$$

$$\begin{aligned} \mathcal{B} = & \frac{Eh}{2(1-\upsilon^2)}\left(w_{,y}^3 + w_{,y}w_{,x}^2\right) + \frac{(3C_{111} - 2C_{222})h}{4}w_{,x}^2 w_{,y}^3 \\ & + \frac{h}{8}C_{222}w_{,y}^5 + \frac{(3C_{222} - 2C_{111})h}{8}w_{,x}^4 w_{,y}, \end{aligned} \tag{9b}$$

$$\mathcal{C}_{,xx} = \frac{Eh^3}{12(1+\upsilon)}\left(w_{,xxxx} + w_{,xxyy}\right) + \frac{Eh^3\upsilon}{12(1-\upsilon^2)}w_{,xxxx}, \tag{9c}$$

$$\mathcal{D}_{,yy} = \frac{Eh^3}{12(1+\upsilon)}\left(w_{,yyyy} + w_{,xxyy}\right) + \frac{Eh^3\upsilon}{12(1-\upsilon^2)}w_{,yyyy}, \tag{9d}$$

$$\mathcal{F}_{,xy} = \frac{Eh^3\upsilon}{6(1-\upsilon^2)}w_{,xxyy}. \tag{9e}$$

These equations should be solved with the boundary conditions of the plates (Ansari et al. 2012):

simply supported edges

$$\begin{aligned} & w = 0;\ w_{,xx} + \upsilon w_{,yy} = 0;\ \upsilon w_{,xx} + w_{,yy} = 0 \text{ at } x \\ & \quad = 0, a \text{ and } y = 0, b, \end{aligned} \tag{10}$$

rigidly clamped edges

$$w = 0; \quad w_{,x} = 0; \quad w_{,y} = 0 \text{ at } x = 0, a \text{ and } y = 0, b. \tag{11}$$

3 Solution using Galerkin's method

Equation (8) and the simply supported or rigidly clamped boundary condition (10, 11) form a high order ordinary differential equation whose exact solution is almost impossible to obtain. Therefore, the Galerkin's method is used to solve this nonlinear system approximately.

Consider L the nonlinear differential operator (Chia 1980), whose expression is given by the left hand side of Eq. (8), namely

$$\begin{aligned} L(w) = & \mathcal{A}_{,x} + \mathcal{B}_{,y} - \mathcal{C}_{,xx} - \mathcal{D}_{,yy} - \mathcal{F}_{,xy} - mh\ddot{\omega} \\ & + m\frac{h^3}{12}\ddot{\omega}_{,xx} + m\frac{h^3}{12}\ddot{\omega}_{,yy}. \end{aligned} \tag{12}$$

Thus Eq. (8) can be re-written as

$$L(w) = 0. \tag{13}$$

The approximate solution of Eq. (13) is taken to be

$$w = \sum_{m=1}^{M}\sum_{n=1}^{N} A_{mn}(t)\Phi_{mn}(x, y), \tag{14}$$

where $A(t)$ are variable coefficients to be determined and $\Phi(x, y)$ are suitably chosen functions which have to satisfy the prescribed boundary conditions and be capable of illustrating the mode of deformation.

By the use of Galerkin's method, the following equation must hold (Chia 1980),

$$\iint_A L(w)\Phi_{mn}(x,y)dxdy = 0. \tag{15}$$

Simultaneously consideration of geometrically nonlinear elasticity and material nonlinearity adds significant difficulty in analysis. Therefore, in this paper, we solve the problem by one-term approximate, namely $M = N = 1$. In such case, what we obtain is the fundamental frequency for the first mode of vibration. The first mode vibration is the most representative vibration case, a well cognition of how the material nonlinearity and geometric nonlinearity impact the first mode vibration can efficiently explain the effect of nonlinear elasticity and nonlinear geometry. Moreover, the first mode is easy to solve. Because of the validity and facility, we only considered the first mode vibration. The result is instrumental in the further study of the vibration behavior of the plates at small scale.

3.1 Simply supported edges

By one-term approximate, let (Wei et al. 2009)

$$\Phi_{11}(x,y) = \sin\frac{\pi x}{a}\sin\frac{\pi y}{b}. \tag{16}$$

Accordingly, the corresponding deflection is

$$w = A(t)\sin\frac{\pi x}{a}\sin\frac{\pi y}{b}, \tag{17}$$

which obviously satisfies the simply supported edges boundary in Eq. (10). Equation (15) can be reduced to

$$\iint_A L(w)\Phi_{11}(x,y)dxdy = 0. \tag{18}$$

Upon substituting (12) and (16) into (18) and performing the integration, we obtain

$$\lambda_1\ddot{A} + \lambda_2 A + \lambda_3 A^3 + \lambda_4 A^5 = 0, \tag{19}$$

where

$$\lambda_1 = \frac{1}{4}mh\left(1 + \frac{h^2}{12}\frac{\pi^2}{a^2} + \frac{h^2}{12}\frac{\pi^2}{b^2}\right), \tag{20a}$$

$$\lambda_2 = \frac{\pi^4 Eh^3}{48(1-\upsilon^2)}\left(\frac{1}{a^2} + \frac{1}{b^2}\right)^2, \tag{20b}$$

$$\lambda_3 = \frac{\pi^4 Eh}{128(1-\upsilon^2)}\left(\frac{9}{a^4} + \frac{9}{b^4} + \frac{2}{a^2b^2}\right), \tag{20c}$$

$$\lambda_4 = \frac{\pi^6 h}{2048}\left\{\frac{3}{a^2b^2}\left[\left(\frac{3}{b^2} - \frac{2}{a^2}\right)C_{111} + \left(\frac{3}{a^2} - \frac{2}{b^2}\right)C_{222}\right] + \frac{25}{a^6}C_{111} + \frac{25}{b^6}C_{222}\right\}. \tag{20d}$$

In Eq. (19), the term $\lambda_3 A^3$ are caused by the Von Karman nonlinear strain, if we do not consider the geometry nonlinearity, this term will vanish; the term $\lambda_4 A^5$ are caused by the second order nonlinear elasticity, when $C_{111} = C_{222} = 0$, the model reduce to a linear elastic problem.

Equation (19) is a non-linear second-order differential equation. It does not admit an exact solution. However, we can employ the harmonic balance method to obtain an approximate solution. The solution result will be demonstrated in Sect. 4.

3.2 Rigidly clamped edges

The same procedure with simply supported edges will be applied. We let (Jomehzadeh and Saidi 2011)

$$\Phi_{11}(x,y) = \sin^2\frac{\pi x}{a}\sin^2\frac{\pi y}{b}, \tag{21}$$

which obviously satisfies the rigidly clamped edges boundary in Eq. (11). The corresponding deformation of the plate is

$$w = A(t)\sin^2\frac{\pi x}{a}\sin^2\frac{\pi y}{b}. \tag{22}$$

In this case, Eq. (15) reduces to

$$\iint_A L(w)\Phi_{11}(x,y)dxdy = 0. \tag{23}$$

Upon substitution of Eq. (12) and (21) into Eq. (23), we obtain

$$\lambda_1\ddot{A} + \lambda_2 A + \lambda_3 A^3 + \lambda_4 A^5 = 0, \tag{24}$$

where

$$\lambda_1 = \frac{9}{64}mh\left(1 + \frac{h^2}{9}\frac{\pi^2}{a^2} + \frac{h^2}{9}\frac{\pi^2}{b^2}\right), \tag{25a}$$

$$\lambda_2 = \frac{\pi^4 Eh^3}{16(1-\upsilon^2)}\left(\frac{1}{a^4} + \frac{1}{b^4} + \frac{2}{3}\frac{1}{a^2b^2}\right), \tag{25b}$$

$$\lambda_3 = \frac{5\pi^4 Eh}{2048(1-\upsilon^2)}\left(\frac{21}{a^4} + \frac{21}{b^4} + \frac{10}{a^2b^2}\right), \tag{25c}$$

$$\lambda_4 = \frac{\pi^6 h}{65536}\left\{\frac{1}{a^2b^2}\left[\left(\frac{1323}{b^2} - \frac{882}{a^2}\right)C_{111} + \left(\frac{1323}{a^2} - \frac{882}{b^2}\right)C_{222}\right] + \frac{1155}{2a^6}C_{111} + \frac{1155}{2b^6}C_{222}\right\}. \tag{25d}$$

The same with simple supported edges, in Eq. (24), the term $\lambda_3 A^3$ are caused by the Von Karman nonlinear strain, if we do not consider the geometry nonlinearity, this term will vanish; the term $\lambda_4 A^5$ are caused by the second order nonlinear elasticity, when $C_{111} = C_{222} = 0$, the model reduce to a linear elastic problem.

Equation (24) has the same form of Eq. (19). The only difference is that the coefficients λ_1, λ_2, λ_3, λ_4 have different values. Consequently, the solution of Eq. (24) possesses the same form with the solution of Eq. (19), the result will also be shown in Sect. 4.

4 Results and discussions

Graphene is a typically plate-like structure, we use the graphene as a case to discuss the result. The full set of third-order elastic constants of graphene was reported as $C_{111} = -1689.2\,\mathrm{N\,m^{-1}}$, $C_{222} = -1487.7\,\mathrm{N\,m^{-1}}$, $C_{112} = -484.1\,\mathrm{N\,m^{-1}}$, C_{111} is different than C_{222} while taking the nonlinear features into account (Jomehzadeh and Saidi 2011). In what follows, the method of harmonic balance (Chia 1980) with one-term approximation

$$A = A_0 \cos \omega t \tag{26}$$

is employed. As a result,

$$\ddot{A} = -\omega^2 A_0 \cos \omega t \tag{27}$$

With the substitution of Eqs. (26, 27) into Eqs. (19) and (24), we obtain

$$\left(-\lambda_1\omega^2 + \lambda_2 + \frac{3}{4}\lambda_3 A_0^2 + \frac{5}{8}\lambda_4 A_0^4\right)\cos \omega t + \textit{high order harmonics} = 0. \tag{28}$$

According to harmonic balance, by setting the coefficient of $\cos \omega t$ equal to zero, Eq. (28) permits the following solution

$$\omega^2 = \omega_0^2 + \frac{3}{4}\frac{\lambda_3}{\lambda_1}A_0^2 + \frac{5}{8}\frac{\lambda_4}{\lambda_1}A_0^4, \tag{29}$$

or

$$\frac{\omega^2}{\omega_0^2} = 1 + \frac{3}{4}\frac{\lambda_3}{\lambda_2}A_0^2 + \frac{5}{8}\frac{\lambda_4}{\lambda_2}A_0^4, \tag{30}$$

where $\omega_0^2 = \frac{\lambda_2}{\lambda_1}$ is the free vibration frequency of a linear elastic plate.

In order to discuss the vibration frequencies of different shaped plates, the aspect ratio $\xi = a/b$ and the thickness-length ratio $\eta = h/a$ are introduced. Substitute the corresponding values of λ_1, λ_2, λ_3, λ_4 into Eq. (19) or (24), for simply supported edges, the vibration frequency is

$$\left(\frac{\omega^2}{\omega_0^2}\right)_{SS} = 1 + \varphi_{SS}\left(\frac{A_0}{h}\right)^2 - \psi_{SS}\left(\frac{A_0}{h}\right)^4\eta^2, \tag{31a}$$

$$\varphi_{SS} = \frac{3}{4}\frac{3\left(9 + 2\xi^2 + 9\xi^4\right)}{8\left(1+\xi^2\right)^2}, \tag{31b}$$

$$\psi_{SS} = -\frac{5}{8}\frac{3\pi^2\left(1-\upsilon^2\right)\left\{3\xi^2\left[\left(3\xi^2-2\right)C_{111} + \left(3-2\xi^2\right)C_{222}\right] + 25C_{111} + 25\xi^6 C_{222}\right\}}{128E\left(1+\xi^2\right)^2}, \tag{31c}$$

and, for rigidly clamped edges, the vibration frequency is

$$\left(\frac{\omega^2}{\omega_0^2}\right)_{RC} = 1 + \varphi_{RC}\left(\frac{A_0}{h}\right)^2 - \psi_{RC}\left(\frac{A_0}{h}\right)^4\eta^2, \tag{32a}$$

$$\varphi_{RC} = \frac{3}{4}\frac{5\left(21 + 21\xi^4 + 10\xi^2\right)}{128\left(1 + \xi^4 + \frac{2}{3}\xi^2\right)}, \tag{32b}$$

$$\psi_{RC} = -\frac{5}{8}\frac{\pi^2\left(1-\upsilon^2\right)\left\{\xi^2\left[\left(1323\xi^2 - 882\right)C_{111} + \left(1323 - 882\xi^2\right)C_{222}\right] + \frac{1155}{2}C_{111} + \frac{1155}{2}\xi^6 C_{222}\right\}}{4096E\left(1 + \frac{2}{3}\xi^2 + \xi^4\right)}. \tag{32c}$$

In view of Eqs. (31a) and (32a), the terms $\varphi_{SS}\left(\frac{A_0}{h}\right)^2$ and $\varphi_{RC}\left(\frac{A_0}{h}\right)^2$ are caused by the Von Karman nonlinear strain, and the terms $\psi_{SS}\left(\frac{A_0}{h}\right)^4\eta^2$ and $\psi_{RC}\left(\frac{A_0}{h}\right)^4\eta^2$ are caused by the second order nonlinear elasticity. Consequently, both the geometry nonlinearity and the elastic nonlinearity will lead to the dependence of the frequency ratio on the amplitude. More specifically, the geometry nonlinearity increases the frequency ratio while the elastic nonlinearity reduces the frequency ratio. Shown in Table 1 is the value of $\varphi_{SS}\left(\frac{A_0}{h}\right)^2$, $\varphi_{RC}\left(\frac{A_0}{h}\right)^2$, $\psi_{SS}\left(\frac{A_0}{h}\right)^4\eta^2$ and $\psi_{RC}\left(\frac{A_0}{h}\right)^4\eta^2$ when $A_0/h = 1$, $\eta = 0.1$ for varies aspect ratios. It is seem that when the aspect ratio is 1, $\varphi_{SS}\left(\frac{A_0}{h}\right)^2$, $\varphi_{RC}\left(\frac{A_0}{h}\right)^2$, $\psi_{SS}\left(\frac{A_0}{h}\right)^4\eta^2$ and $\psi_{RC}\left(\frac{A_0}{h}\right)^4\eta^2$ have their minimum values, $\varphi_{SS}\left(\frac{A_0}{h}\right)^2 = 1.40625$, $\varphi_{RC}\left(\frac{A_0}{h}\right)^2 = 0.08059$,

Table 1 Value of $\varphi_{SS}\left(\frac{A_0}{h}\right)^2$, $\varphi_{RC}\left(\frac{A_0}{h}\right)^2$, $\psi_{SS}\left(\frac{A_0}{h}\right)^4\eta^2$ and $\psi_{RC}\left(\frac{A_0}{h}\right)^4\eta^2$ when $A_0/h = 1, \eta = 0.1$ for varies aspect ratio

	$\varphi_{SS}\left(\frac{A_0}{h}\right)^2$	$\psi_{SS}\left(\frac{A_0}{h}\right)^4\eta^2$	$\varphi_{RC}\left(\frac{A_0}{h}\right)^2$	$\psi_{RC}\left(\frac{A_0}{h}\right)^4\eta^2$
$\xi = 0.02$	2.52945	0.14381	0.61519	0.03463
$\xi = 0.05$	2.52006	0.14324	0.61494	0.03464
$\xi = 0.2$	2.36483	0.13373	0.61068	0.03475
$\xi = 0.5$	1.81125	0.09700	0.59140	0.03534
$\xi = 1$	1.40625	0.08059	0.57129	0.04581
$\xi = 2$	1.81125	0.38800	0.59140	0.14135
$\xi = 5$	2.36483	3.34328	0.61068	0.86875
$\xi = 20$	2.52006	57.2968	0.61494	13.8552
$\xi = 50$	2.52945	359.519	0.61519	86.5778

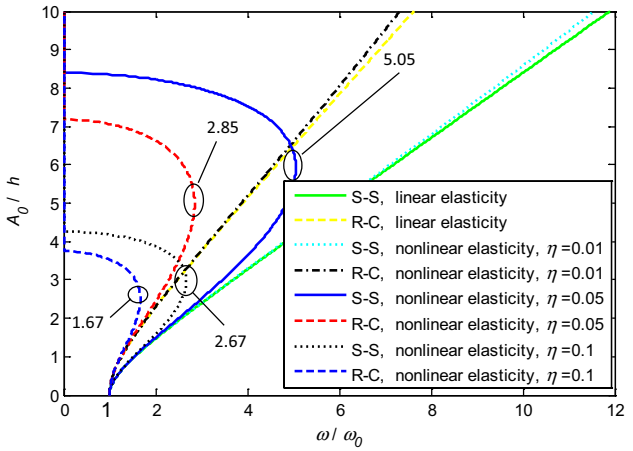

Fig. 2 Relationship between vibration frequency and amplitude for simply supported (S–S) and rigidly clamped (R–C) plate ($\upsilon = 0.3$)

$$\psi_{SS}\left(\frac{A_0}{h}\right)^4\eta^2 = 0.57129 \quad \text{and} \quad \psi_{RC}\left(\frac{A_0}{h}\right)^4\eta^2 = 0.04581.$$

As the aspect ratio increases over 20, $\psi_{SS}\left(\frac{A_0}{h}\right)^4\eta^2$ and $\psi_{RC}\left(\frac{A_0}{h}\right)^4\eta^2$ increase sharply, when the aspect ratio is 50, those two terms are up to 359.519 and 86.5778, respectively. To conclude, the effect of the nonlinear elasticity on the frequency ratio of elastic nonlinearity is smaller than that of the geometry nonlinearity when aspect ratio is less than 5, while the elastic nonlinearity has a steep increasingly effect than geometry nonlinearity when the aspect ratio is larger than 5.

If let $C_{111} = C_{222} = C_{112} = 0$, we can get the frequency of the linear elastic plate $\left(\frac{\omega^2}{\omega_0^2}\right)_{RC} = 1 + \varphi_{RC}\left(\frac{A_0}{h}\right)^2$, in

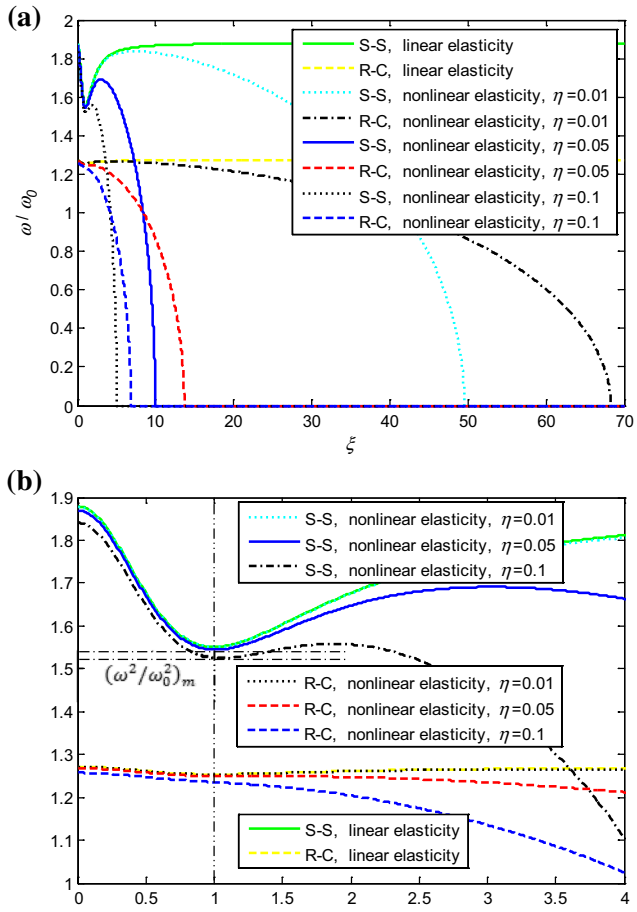

Fig. 3 Vibration frequency under different values of ξ for simply supported (S–S) and rigidly clamped (R–C) plate ($\upsilon = 0.3$, $\frac{A_0}{h} = 1$) for **a** $0 < \xi < 70$; for **b** $0 < \xi < 4$

which we can find that the free vibration frequency ratio of the linear elastic plate is independent of thickness-length ratio. The free vibration frequency of the square plate can be determined by setting $\xi = 1$.

Comparison of the simply supported boundary and the rigidly clamped boundary for square plate for $\upsilon = 0.3$ is shown in Fig. 2. The green and yellow lines stand for the simple supported and rigidly clamped linear elastic graphene sheet, respectively. The relationship between the frequency ratio and the amplitude is almost linear. When considering the nonlinear elasticity, the frequency ratio has a peak value for both the simple supported and rigidly clamped graphene sheet, the larger the thickness-length ratio is, the smaller the peak value is. The values for the particular case are shown in Fig. 2.

The vibration frequency for different values of ξ for simply supported and rigidly clamped plates for

Table 2 The minimal value of $\left(\omega^2/\omega_0^2\right)_m$ and corresponding stagnation point for varies thickness-length ratio when $A_0/h = 1$

	$\left(\omega^2/\omega_0^2\right)_m$	Corresponding stagnation point (ξ)
$\eta = 0.1$	1.52436	1.012317
$\eta = 0.05$	1.54467	1.003093
$\eta = 0.02$	1.55017	1.000496
$\eta = 0.01$	1.55094	1.000124
$\eta = 0.001$	1.55121	1.000001239
Elasticity	1.55121	1

$\upsilon = 0.3, A_0/h = 1$ is shown in Fig. 3a. It is seen that the thickness-length ratio has an obvious effect of the vibration frequency: as the thickness-length ratio increases, the frequency ratio decreases. For simply supported plate, the frequency ratio has an evident minimal value $\left(\omega^2/\omega_0^2\right)_m$ when ξ is approximately equal to 1. The minimum values of $\left(\omega^2/\omega_0^2\right)_m$ and corresponding stagnation points for varies thickness-length ratios when $A_0/h = 1$ are listed in Table 2. From Table 2 we can find that the elastic nonlinearity will reduce the value of $\left(\omega^2/\omega_0^2\right)_m$ and the thickness-length ratio has an influent on such effect: when the thickness-length ratio decreases, $\left(\omega^2/\omega_0^2\right)_m$ gradually approach to the linear elastic plate. On the other hand, for rigidly clamped plate, there is no obvious minimal value (see in Fig. 3b). It can be checked by finding the stagnation point of Eq. (31a) for ξ. By setting $\frac{\partial}{\partial\xi}\left(\frac{\omega^2}{\omega_0^2}\right)_{SS} = 0$, we can easily get $\xi_{SS} = \sqrt{1+\phi_{SS}}$, where

$$\phi_{SS} = -\frac{15\pi^2\left(1-\upsilon^2\right)}{24576E}\Delta_{SS}\left(\frac{A_0}{h}\right)^2\eta^2, \tag{33a}$$

$$\Delta_{SS} = \left(48\xi^2 - 112\right)C_{111} + \left(18 - 42\xi^2 + 150\xi^4 + 50\xi^6\right)C_{222}. \tag{33b}$$

When $\xi = 1$, ϕ_{SS} is $2.47851\left(\frac{A_0}{h}\right)^2\eta^2$. If the elastic nonlinearity is not considered, the stagnation point is precise equal to 1. When thickness-length ratio is 0.1, the stagnation point is 1.012317. Recall that$\xi = 1$ stand for the graphene sheet is square shaped, we can draw the conclusion that if only take the geometry nonlinearity into consider, a square plate possesses the lowest free vibration frequency. If considering the elastic nonlinearity in the same time, the graphene sheet whose aspect ratio is $\sqrt{1+\phi_{SS}}$ possesses the lowest free vibration frequency. As the thickness-length ratio decreases, the aspect ratio of which has the lowest free vibration frequency approach to 1 gradually. When the thickness-length down to 0.01, the aspect ratio is almost 1.

5 Conclusion

In the present work, free vibration of monolayer graphene sheet under simple supported and rigidly clamped boundary condition has been carried out with continuum model. From the present work following conclusions are drawn:

1. Both the geometry nonlinearity and the elastic nonlinearity will lead to the dependence of frequency ratio on the amplitude. The geometry nonlinearity increases the frequency ratio but the elastic nonlinearity reduces the frequency ratio. The elastic nonlinearity has a less effect on the frequency ratio than the geometry nonlinearity when the aspect ratio of the sheet is less than 5. However, the elastic nonlinearity plays a primary role than geometry nonlinearity when the aspect ratio is larger than 5.
2. The free vibration frequency ratio of a linear elastic graphene sheet has been found to be independent of thickness-length ratio of the sheet. However, the thickness-length ratio has an obvious effect on the nonlinear elastic behavior of the graphene sheet: as the thickness-length ratio increases, the frequency ratio decreases. In addition, the thickness-length ratio has been observed more significant effect on the simple supported plate than on the rigidly clamped plate.
3. For linear elasticity and nonlinear geometry mode, a square graphene sheet possesses the lowest free vibration frequency. For nonlinear elasticity and nonlinear geometry model, the graphene sheet with a aspect ratio $\sqrt{1+\phi_{SS}}$ possesses the lowest free vibration frequency. As the thickness-length ratio decreases, the aspect ratio corresponding to the lowest free vibration frequency approaches to 1 gradually. When the thickness-length decreases to less than 0.01, aspect ratio is almost 1.

Acknowledgments This research was supported by the Natural Science Foundation of Guangdong Province of China (Project no. 2016A030311006), Research Innovation Fund of Shenzhen City of China (Project no. JCYJ20150805142729431) and the National Natural Science Foundation of China (Project nos. 11172081, 11372086).

References

Ansari R, Gholami R, Shojaei MF, Mohammadi V, Darabi MA (2012) J Eng Mater Technol 134:041013
Arani AG, Ghaffari M, Jalilvand A, Kolahchi R (2013) Acta Mech 224:3005–3019
Asghari M (2012) Int J Eng Sci 51:292–309
Behfar K, Naghdabadi R (2005) Compos Sci Technol 65:1159
Cadelano E, Palla PL, Giordano S, Colombo L (2009) Phys Rev Lett 102:235502
Chia C (1980) Nonlinear analysis of plates. McGraw-Hill International Book Company
Farokhi H, Ghayesh MH (2015) Int J Mech Sci 90:133–144
Ghayesh MH, Farokhi H (2015) Int J Eng Sci 86:60–73

Jomehzadeh E, Saidi A (2011a) Compos Struct 93:1015
Jomehzadeh E, Saidi A (2011b) Comp Mater Sci 50:1043
Lee C, Wei X, Kysar JW, Hone J (2008) Science 321:385
Sahmani S, Bahrami M (2015) J Mech Sci Technol 29:1151–1161
Sfyris D, Sfyris G, Galiotis C (2014) Int J NonLinear Mech 67:186
Wang K, Wang B (2012) J Appl Phys 112:013520
Wei X, Fragneaud B, Marianetti CA, Kysar JW (2009) Phys Rev B 80:205407
Xiao T, Xu X, Liao K (2004) J Appl Phys 95:8145
Yang X, Lim CW (2009) Sci China Ser E 52:617
Yang J, Ke L, Kitipornchai S (2010) Phys E 42:1727